

3D Modeling based on Current Continuity for STM Carrier Profiling of Semiconductor Devices

Koichi Fukuda¹, Masayasu Nishizawa^{1*}, Tetsuya Tada¹, Leonid Bolotov²,
Kaina Suzuki³, Shigeo Sato³, Hiroshi Arimoto¹, and Toshihiko Kanayama¹

¹ Nanodevice Innovation Research Center (NIRC), National Institute of Advanced Industrial Science and Technology (AIST),
16-1 Onogawa, Tsukuba, Ibaraki 305-8569, Japan Phone: +81-29-849-1565

² Institute of Applied Physics, University of Tsukuba, 1-1-1 Tennodai, Tsukuba, Ibaraki 305-8573, Japan

³ Fujitsu Semiconductor Ltd., 50 Fuchigami, Akiruno, Tokyo 197-0833, Japan

Abstract— Current continuity based 3D modeling of STM carrier profiling of semiconductor devices is achieved for the first time. Tunnel currents between probe tip and devices are solved consistently with current continuity consideration. It is revealed that tunnel current is reduced in current continuity model under depletion conditions. Spatial resolution achieved in the model is discussed in comparison to potential based modeling. Influence of discrete dopants is also discussed in concern with Coulomb potential fluctuations in nanoscale systems, which is a key issue of nano devices.

I. INTRODUCTION

Carrier profiling becomes a major issue in developing semiconductor devices of nanometer dimensions. Profiling of device cross sections by scanning tunneling microscopy (STM) has been studied already [1][2][3]. Fig.1 shows an example of STM measurement across a p-n junction. Carrier distribution is deduced from change in STM *IV*-curves depending on the measured points. STM can detect individual dopant atoms locating just beneath the surface [3].

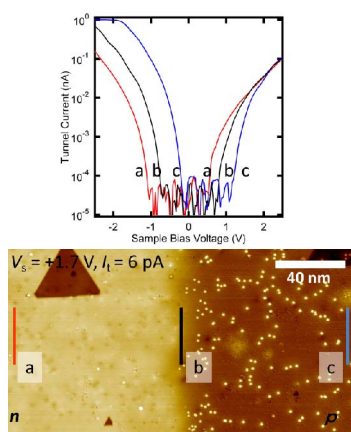


Fig. 1 STM I-V curves across a p-n junction [3]. 3 curves are for indicated positions in the plane image.

Principle of STM carrier profiling is schematically shown in fig.2. The tip-sample distance is automatically adjusted by maintaining constant tunneling current at a specified setpoint voltage. Since the applied voltage modifies potential of the sample surface just beneath the tip, STM simulation is indispensable for quantitative carrier profiling.

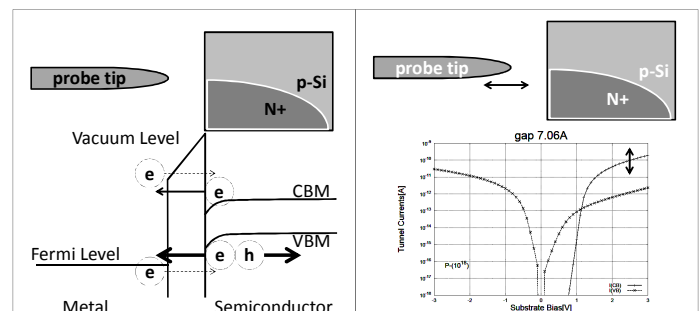


Fig.2 Band diagram between the probe tip and sample for $V_{sub} < 0$ and the tunneling mechanisms (left). The calculated *IV*-curve with a setpoint of $V_{sub} = 2.5V$ and $I_t = 0.1nA$ (right).

3D modeling of STM has been progressed by potential-based approach [4], in which tunnel current and potential distribution were separately calculated and current flow in the sample was completely neglected. This paper presents a new approach considering current continuity.

II. NUMERICAL SIMULATION OF TUNNELING CURRENT

TCAD system HyENEXSS[5] is used for 3D simulation as shown in fig.3. Tunneling from and into semiconductor conduction and valence bands are considered. Not only tip induced band bending [6] but also carrier continuity inside semiconductor is automatically included by the device simulation. The STM probe tip is treated as a device structure in our simulations. Tip-sample distances are automatically adjusted similar to the realistic STM measurements.

*) Current address Research Institute of Biomolecule Metrology Co., Ltd.

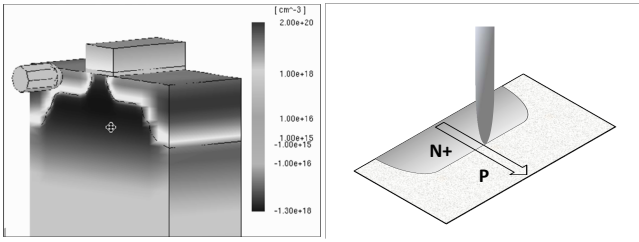


Fig.3 A 3D structure of an STM probe tip and a semiconductor sample created by HyENEXSS (left). Illustration of carrier profiling across a PN junction (right).

III. SIMULATION OF P-N JUNCTION

To demonstrate the ability of the 3D current continuity modeling, STM measurements along a line across an N⁺/P junction are simulated for dopant concentrations of 10^{18} cm^{-3} for p-type and 10^{20} cm^{-3} for n-type regions as shown in the right illustration of fig.3. Fig.4 shows *IV* curves calculated at a distance of 0.2 μm sufficiently far from the N/P junction where the tip-sample distance was set with the tunnel current $I_t=0.1\text{nA}$ at a substrate voltage $V_{\text{sub}}=2.5\text{V}$. Contributions of the tunneling current components associated with conduction band (CB) and valence band (VB) tunneling are identified. We note that under $V_{\text{sub}} < 0\text{V}$, the valence band tunneling dominates in both the models. However, for the current continuity model the VB current is slightly smaller due to the difference in carrier distribution. It should be mentioned that this tip position is out of the depletion region of the N/P junction in this example. Thus, different results are obtained from these models even at thermal equilibrium positions.

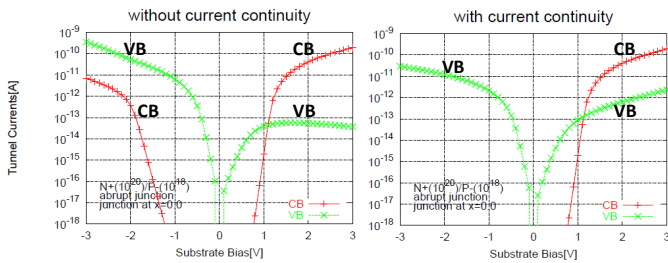


Fig.4 STM *IV* curves at $10^{18} [1/\text{cm}^3]$ p-type 0.2 μm far from the N⁺/P junction. 2 curves are associated with conduction band (CB) and valence band (VB) tunneling.

Potential and carrier profiles along the semiconductor surface of the same configuration at $V_{\text{sub}}=-2.5\text{V}$ are shown in fig.5. Hole concentration just below the probe tip center (0.2 μm) of current continuity based model (right) is larger than potential based results (left), while electron concentration is reduced in turn. Both of these differences are caused by flow of tunneling currents inside the semiconductor, especially hole currents increase potential slope in the high resistivity depletion region which is caused by the tip potential around 0.2 μm .

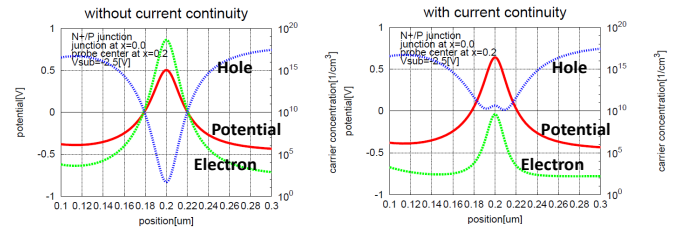


Fig.5 Potential and carrier profiles along the semiconductor surface at $V_{\text{sub}}=-2.5\text{V}$ of fig.4. Left figure is results of potential-based calculations, and right figure represents current continuity results.

We compare *IV* curves calculated for different distances to the N/P junction in fig.6. Shapes of the curves change depending on the distance from the junction.

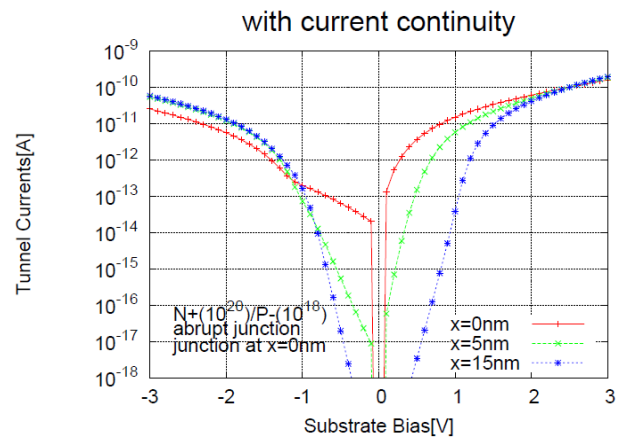


Fig.6 *IV*-curves at different distances from N⁺/P junction.

Fig.7 shows tunneling currents flow in the depletion region depending on carrier concentration around the tips center; electrons to N⁺ and holes to P- region. Microscopic behavior of carriers inside semiconductor is important to understand the measured results especially near the N/P junctions. Such effects are automatically considered by our current continuity approach in principle.

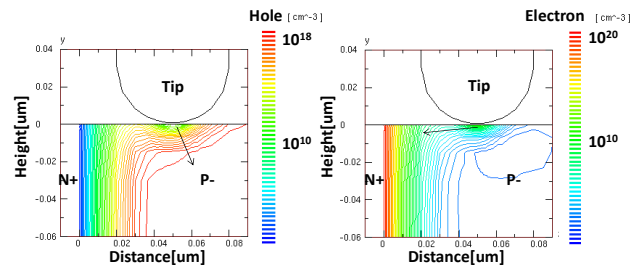


Fig.7 Hole (left) and electron (right) concentration below the probe tips for $V_{\text{sub}}=-2.5\text{V}$ condition. Both carrier concentrations are low because of current continuity constraints.

To discuss potential profiles, it is constructive to consider the influence of the STM tip radius. Similarly to the STM data in fig. 1, we calculate the onset voltage as a function of distance to the junction (fig.8). In the case of 30 nm tip radius (right), onset voltage profiles in depletion conditions ($V_{sub} < 0$) match better to the reference potential than the 100nm tip radius case. Thus, the accuracy of measured potential profile can be examined in detail by the present method.

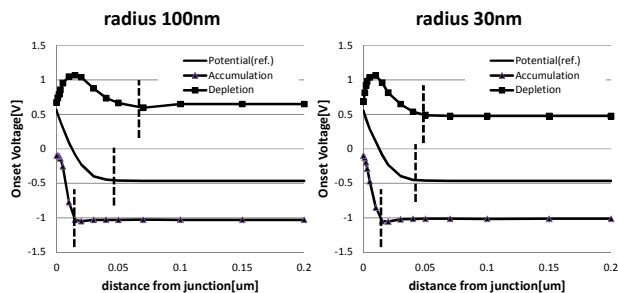


Fig.8 Onset voltage plotted as a function of distance from PN junction for tip radius of 100nm (left) and 30nm (right).

IV. DISCRETE DOPANT EFFECT

To evaluate the spatial resolution of the model simulations, discrete dopant effects are investigated by introducing either screened long-range configurations of Coulomb potential or nearest grid point potential [7][8][9]. Fig.9 is a snapshot of the simulated electrostatic potential distribution considering random discrete dopants for the nearest grid point configuration.

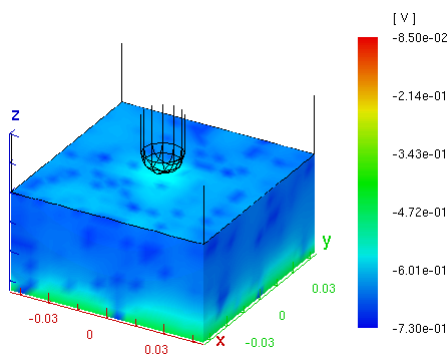


Fig.9 An example of the potential distribution including discrete dopants.

It has been pointed out that, Coulomb potential of a discrete dopant is so broad that it is inadequate to assign its charge to a very small discretization mesh in device simulations[7]. In case of carrier transport calculation such as

in standard device simulation, it has been proposed to treat the dopant charge considering the screening length [7].

Contour maps of onset voltages, corresponding to the substrate bias at $I_t=10^{-13}$ A, obtained in both the screened Coulomb and nearest grid models are shown in fig.10. Although the onset voltage maps are different from the STM images shown in fig.1, they are similarly sensitive to the discrete dopant positions. In case of STM measurements for very fine spatial resolutions, the tunneling current is sensitive to strong short range component of the Coulomb potential. For such a purpose, the nearest grid point assignment seems to be more adequate.

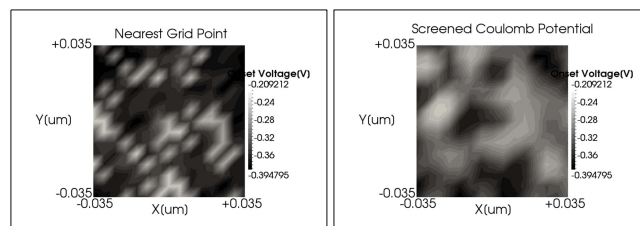


Fig.10 Contour map of tunnel current onset voltages by simulation of nearest grid point method (left) and screened long range Coulomb (right).

Previously, we have reported on observation of boron and arsenic dopant atoms in Si under different bias voltages as shown in fig.11[3]. The white arrows in the figure indicate boron ions which are observed bright in (a) $V_{sub} < 0$ and dark in (b) $V_{sub} > 0$. The surface conditions of carrier distribution are affected by the potential difference between the substrate and the probe tip. The image in fig.11(a) corresponds to a depletion condition while that in (b) is an accumulation condition for the p-type region. It is noticeable that the sizes of the boron-ion images are almost identical in both the conditions. This fact shows that the screened long range components of the Coulomb potential, which change drastically depending on carrier concentration around the boron ion, does not strongly affect the tunneling currents in case of STM measurements. Consequently the tunneling currents are affected mainly by the short range component of the Coulomb potential which does not change so much depending on the carrier concentrations.

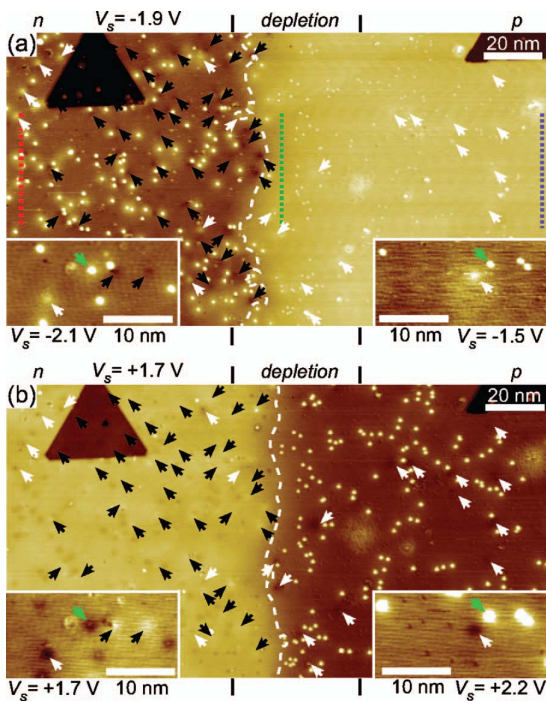


Fig.11 STM images of the PN-junction using (a) $V_{\text{sub}}=-1.9\text{V}$ and (b) $V_{\text{sub}}=+1.7\text{V}$ conditions [3]. The white arrows indicate the position of boron and the black arrows indicate arsenic.

V. CONCLUSIONS

Current-continuity-based 3D modeling of STM carrier profiling of semiconductor devices is presented. Consideration of current continuity reveals that the tunnel current in depletion conditions is reduced compared with potential based modeling. The present model enables detailed discussions of spatial resolution and discrete dopant effects. Discrete dopants affect the STM tunneling current mainly by strong short range components of Coulomb potential in accord with experimental STM data.

ACKNOWLEDGMENT

We thank Professor Nobuyuki Sano of University of Tsukuba for fruitful discussions concerning the discrete dopant effects.

- [1] H. Fukutome, T. Aoyama, and H. Arimoto, IEDM 2001
- [2] H. Fukutome, H. Arimoto, S. Hasegawa, and H. Nakashima, *J. Vac. Sci. Technol. B*22, (2004) 358
- [3] M. Nishizawa, L. Bolotov, and T. Kanayama, *Applied Physics Letters* 90, (2007) 122118
- [4] M. Nishizawa, L. Bolotov, T. Tada, H. Fukutome, H. Arimoto, and T. Kanayama, SSDM 2010.
- [5] HyDeLEOSTM, ver.4.2, Selete, 2007
- [6] R. M. Feenstra, and J. A. Stroscio, *J. Vac. Sci. Technol. B*5 (1987) 923.
- [7] N. Sano et al, *Microelectronics Reliability*, 42 (2002) 189.
- [8] A. Asenov, *IEEE TED* 45 (1998) 2505.
- [9] M.F. Bukhori, S. Roy, and A. Asenov, *Microelectronics Reliability*, 48 (2008) 1549.